AJNR

Three-dimensional MR of the inner ear with steady-state free precession.

C R Guirado, P Martínez, R Roig, F Mirosa, J Salmerón, F Florensa, M Roger and Y Barragón

Three-dimensional MR of the Inner Ear with Steady-State Free Precession

C. R. Guirado, P. Martínez, R. Roig, F. Mirosa, J. Salmerón, F. Florensa, M. Roger, and Y. Barragán

PURPOSE: To describe the steady-state free-precession MR sequence and its application to the study of the inner ear. **METHOD:** The inner ear was imaged with CT and a 0.5-T MR unit in three dimension, to evaluate the various signals from the lumen of the labyrinth. **RESULTS:** Normally, the signal from the perilymphatic and endolymphatic spaces is homogeneous. However, among our cases of neurosensory deafness, differences of signal and morphology were seen in patients with otosclerosis, ossifying labyrinthitis, and inner ear malformations. **CONCLUSION:** Three-dimensional MR, used together with routine two-dimensional fast spin-echo, is another diagnostic tool that can provide new data in the evaluation of the normal and unhealthy inner ear.

The development of magnetic resonance (MR) has been accompanied by sequences that are most useful in the study of the inner ear (1–3). In this article, we set out our experience in the three-dimensional evaluation of the inner ear, using the steady-state free-precession (SSFP) sequence (4, 5).

We report a series of patients with neurosensory hearing loss previously routinely studied with computed tomography (CT) and MR fast spin-echo sequences. In a particular group of adult patients, we made a comparative study with the SSFP sequence.

Patients and Methods

We studied a group of 30 patients with neurosensory hearing loss in whom, in addition to our routine CT and MR protocols, we used the 3-D SSFP sequence using a 0.5-T MR unit with its associated workstation.

The SSFP sequence, which is heavily T2 weighted, is the method of choice to study fluids of low velocity, as is the case with the perilymphatic and endolymphatic spaces (6).

In the SSFP sequence, each excitation pulse serves as the refocusing pulse for the previous excitation. In SSFP, τ equals repetition time, so the echo appears at $2 \times$ repetition time. Because it is not possible to apply a pulse and listen for an echo at the same time, gradients are applied to shift the formation of the echo and make refocusing occur 9 milliseconds before the third excitation pulse. This gradient refocusing introduces some sensitivity to susceptibility and chemical shift artifacts as well as some inhomogeneity effects. These effects are less detrimental than the effects associated with refocused free induction decay sequences for equal echo times. Thus, SSFP provides heavily T2-weighted images, using long echo times, without the effects of long-echo-time, free induction decay–refocused sequences. Because SSFP relies on the formation of a steady state, high rates of flow, such as in the arteries, can produce signal voids (7). This was not, of course, a problem with our inner ear studies. On the other hand, SSFP is very sensitive to pathology, as we have found. We used a matrix of 256×256 or 512×512, using a head coil with a field of view of 24 cm or a surface coil with a field of view of 14 to 18 cm, with a section thickness of 1 mm, without interspaces. Repetition time was 50 milliseconds; echo time was longer than repetition time and was automatically calculated. Flip angle was 20°. This is a 3-D volume acquisition, with 3-D reconstruction. Acquisition time is 14 minutes 34 seconds, with a matrix of 256×256.

We used a workstation that allows us to clean up the image of the labyrinth, removing artifacts produced by neighboring structures such as the temporal lobe and, occasionally, the pathologic signals produced by inflammatory diseases of the middle ear.

Fig 1. Millimetric 3-D reconstruction of the membranous labyrinth with SSFP sequences. *C* indicates cochlea; *v*, vestibule; *ssc*, superior semicircular canal; *psc*, posterior semicircular canal; *lsc*, lateral semicircular canal; and *cc*, crus commune.

Fig 2. Image of the membranous labyrinth shows the vestibular aqueduct (*arrow*).
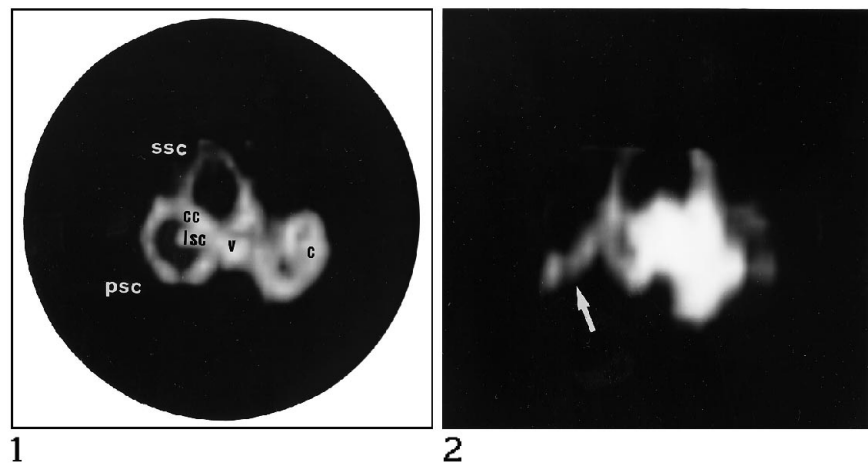
Results

Images of sufficient technical quality were obtained to enable the recognition of the two and one-half turns of the cochlea. Similarly, we could visualize the posterior labyrinth with the vestibule and the semicircular canals (lateral, superior, and posterior) joined by the crus commune (Fig 1). It was possible to see the high signal produced by the ampullae of the semicircular canals, and in some cases, the vestibular aqueduct can be seen (Fig 2). It also was possible to detect the lack of signal produced by anatomic structures such as the oval and the round windows.

In some cases, we have found it difficult to delineate the upper margin of the superior semicircular canal because of the superimposition of the temporal lobe. We also have found small signal defects in the lower part of the posterior semicircular canal.

We have found clinical applications of the SSFP sequence in four cases of otosclerosis, one case (both sides) of ossifying labyrinthitis, and five cases of malformations of the inner ear (8).

Otosclerosis

It is well known that otosclerotic foci in the osseous cochlea can be well visualized by CT. Cochlear otosclerosis is characterized by bone demineralization in the turns.

With the MR SSFP sequence, we demonstrated the intralabyrinthine otosclerotic foci by reduction of the signal from the labyrinth fluids in the various cochlear turns.

We show a case studied with both CT and 3-D MR. In the CT study, osseous alterations can be seen in the cochlea (Fig 3A), whereas the MR image shows low signal attributable to a lack of

Fig 3. Coronal CT section in a case of otosclerosis. The *arrows* show the demineralization foci around both cochleas.

B, 3-D MR image of the inner ear in the same patient with cochlear otosclerosis. The *arrow* shows the intralabyrinthine foci.
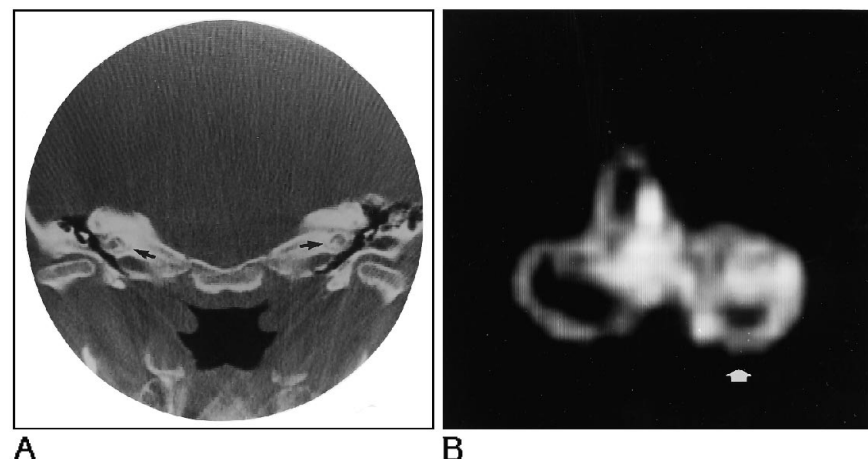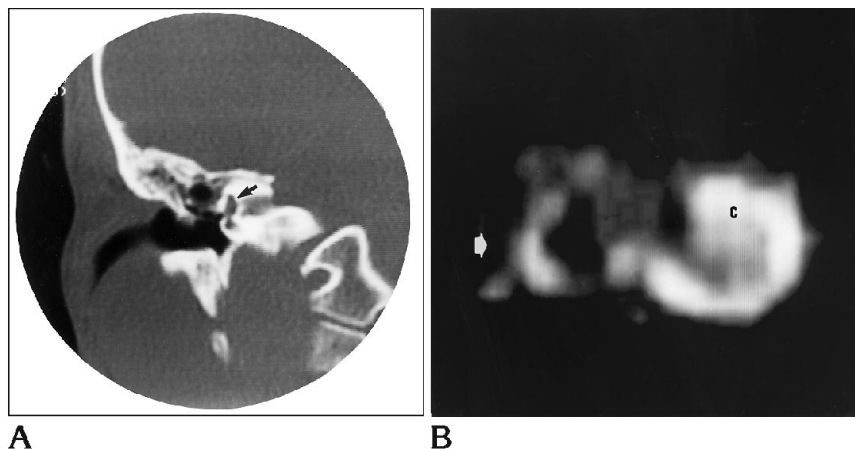
Fig 4. *A*, Coronal CT section in a case of agenesis of the semicircular canals. The *arrow* points to the large vestibule. The semicircular canals are not visible.

B, 3-D reconstruction of the inner ear in the same case. Note the high signal of the cochlea (*c*). The lateral and the superior semicircular canals cannot be seen. The *arrow* shows the low signal of the deformed posterior semicircular canal.

fluid in the perilymphatic and endolymphatic spaces in the same turns (Fig 3B).

The diagnosis of patency of the first turn of the cochlea is of interest in preoperative evaluation of candidates for cochlear implants.

Inner Ear Malformations

We have examined five patients with anomalies in the development of the inner ear with both CT and MR. Among these cases, the most significant were one case of agenesis of the lateral semicircular canal, one case of agenesis of the three semicircular canals, one case of Mondini malformation, and one case of labyrinth dysplasia. Another case showed normal CT anatomy of the labyrinth but with an abnormal signal and configuration of the cochlea on MR.

Agenesis of the Semicircular Canals

The SSFP sequence is complementary to CT, in which only the bone capsule is seen. In a case of agenesis of the semicircular canals, CT showed a large vestibule and absence of development of all three semicircular canals (Fig 4A). The same case was studied with 3-D MR. This showed the vestibule with a very low signal, and some remains of the posterior semicircular canal were recognized.

The normal cochlea stands out with great clarity (Fig 4B).

Mondini Malformation

This anomaly of the cochlea was described by Mondini in 1791 in his doctoral thesis, from a postmortem microscopic examination of a deaf child. He showed there was a dilatation of the vestibule and the lateral semicircular canal. The
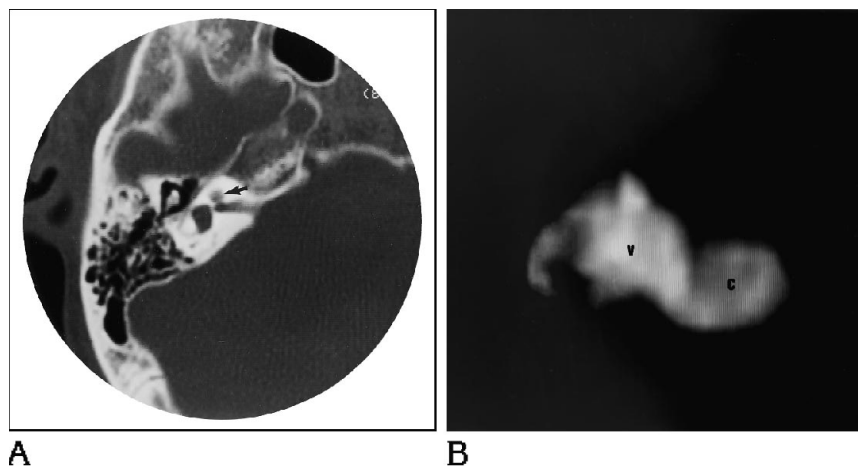

Fig 5. *A*, Axial CT section in a case of Mondini malformation. The *arrow* points to the abnormal development of the cochlea.

B, 3-D MR of the inner ear in the same case. The posterior labyrinth and the cochlea appear dilated. *C* indicates cochlea; and *v*, vestibule.

Fig 6. *A*, Axial CT section of the petrous pyramids in a case of labyrinth dysplasia. The *arrow* shows the severe deformity of the entire labyrinth on the affected side.

B, 3-D MR of the inner ear in the same patient. The entire labyrinth shows severe deformity, with an appearance of balls of cottonwool. The internal auditory canal shows poor differentiation. *C* indicates cochlea; *pl*, posterior labyrinth; *iac*, internal auditory canal, and *v*, vestibule.
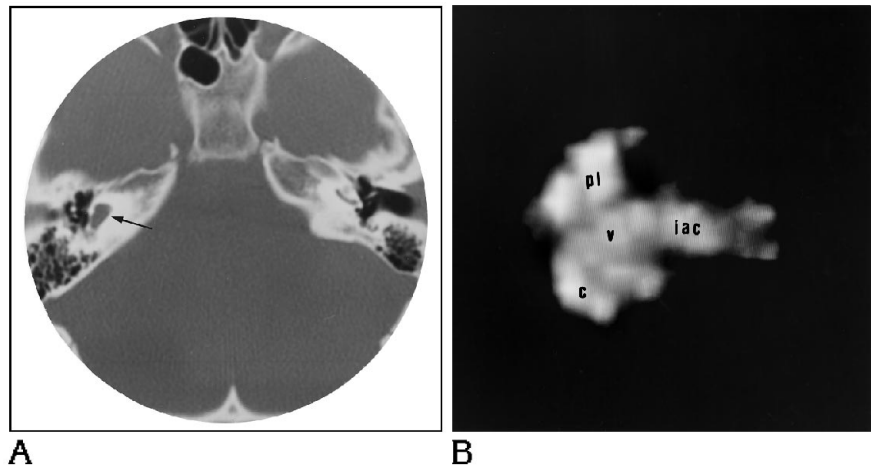
vestibular aqueduct also was dilated. The most significant finding was that the cochlea lacked one of its turns.

These malformations were visible on CT, and no partition walls were visualized in the cochlea (Fig 5A). The MR SSFP sequence creates a 3-D image of the deformity affecting the different parts of the labyrinth, showing the dilatation of the perilymphatic and endolymphatic spaces in the anterior and posterior labyrinth. The incomplete configuration of the cochlea is very clearly seen in the 3-D MR view (Fig 5B).

Labyrinth Dysplasia

This severe malformation is characterized by a general dilatation of the labyrinth and abnormal development of the cochlea observed on CT. The anomaly also affects the internal auditory meatus, which has a characteristic tapering shape (Fig 6A).

3-D MR shows the differences in fluid content in all parts of the labyrinth, with a general appearance that reminded us of balls of cottonwool. However, the signal produced by the internal auditory meatus is very weak (Fig 6B).

Ossifying Labyrinthitis

We present one case of bilateral inner ear lesions previously diagnosed by CT. The deposit of detritus reduces the lumen of the various parts of the labyrinth. CT shows the stenosis of the basal turn of the cochlea, and the semicircular canals are partially obliterated (Fig 7A).

3-D MR shows the true extent of the obliteration or stenosis of the lumen of the labyrinth; this demonstration is important in deciding preoperatively the placement of cochlear implants (Fig 7B).

Fig 7. *A*, Coronal CT section in a case of ossifying labyrinthitis. The *large arrow* shows the stenosis affecting the basal turn of the cochlea, and the *small arrow* shows partial obliteration of the semicircular canals.

B, 3-D MR reconstruction of the inner ear of the same case. The *arrows* show a stenosis of the basal turn of the cochlea.
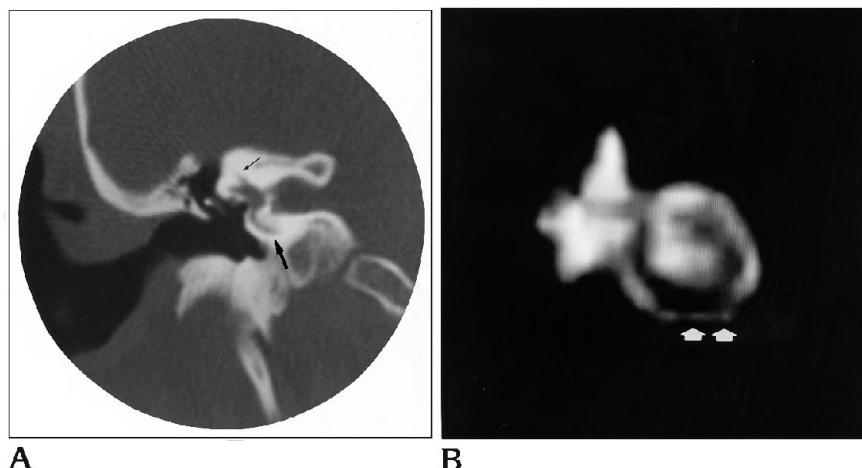
Discussion

The SSFP sequence is another tool in the imaging diagnosis of neurosensory hearing loss. It allows reconstruction of a 3-D "model" of the lumen of the labyrinth, which can be rotated in any plane (9, 10).

In some cases, such as otosclerosis and ossifying labyrinthitis, MR has been shown to be an important method of determining the patency of the cochlear turns as well as their permeability. In cases of malformation, MR of the labyrinth can show abnormal configuration in 3-D. However, patient movement during the rather long imaging time can make 3-D reconstruction impossible.

Interestingly, we have recently identified cases in which reduced signal intensity in the basal turn or the apex of the cochlea corresponded with audiometric findings of high or low pitch deafness, respectively.

Continuing improvement of these techniques is likely to provide direct, noninvasive, topographic diagnosis of cochlear lesions in some kinds of neurosensory deafness.

References

 1. Jackler RK, Dillon WP. Computed tomography and magnetic resonance imaging of the inner ear. *Otolaryngol Head Neck Surg* 1988;99(5):494–504

 2. Brogan M, Chakeres DW, Schmalbrock P. High-resolution 3DFT MR imaging of the endolymphatic duct and soft tissues of the otic capsule. *AJNR Am J Neuroradiol* 1991;12:1–11

 3. Schmalbrock P, Brogan MA, Chakeres DW, Hacker VA, Ying K, Clymer BD. Optimization of submillimeter-resolution MR imaging methods for the inner ear. *Magn Reson Imaging* 1993;3:451–459

 4. Tanioka H, Shirakawa T, Machida T, Sasaki Y. Three-dimensional reconstructed MR imaging of the inner ear. *Radiology* 1991;178:141–144

 5. Stillman AE, Remley K, Loes DJ, Hu X, Latchaw RE. Steady-state free precession imaging of the inner ear. *AJNR Am J Neuroradiol* 1994;15:348–350

 6. Tien RD, Felsberg GJ, Mac Fall J. Three-dimensional MR gradient recalled echo imaging of the inner ear: comparison of FID and echo imaging techniques. *Magn Reson Imaging* 1993;11:429–435

 7. Prorok RJ. Signa Advantage gradient echo pulse sequences: SSFP. *Signa Applications Guide.* Milwaukee, Wis: General Electric; 1990(II):15–17

 8. Pharaboz C, Vignaud J, Le Marec E. MR techniques for the study of the temporal lobe and its environment. *Ann Radiol* 1992;35(1–2):7–15

 9. Marsot-Dupuch K, Meyer B, Falisse B, Nicklaus PA, Chouard CH. 3D imaging of the labyrinth: application to candidates for cochlear implant. *Ann Radiol* 1992;35(1–2):44–49

10. Casselman JW, Kuhweide R, Deimling M, Ampe W, Dehaene I, Meeus L. Constructive interference in steady state 3DFT MR imaging of the inner ear and cerebellopontine angle. *AJNR Am J Neuroradiol* 1993;14:47–57